Optimization of Pneumatic-Cuff based Protocols For Coherent Hemodynamics Spectroscopy

A thesis

submitted by

Namitha Mandayam-Krishnakumar

In partial fulfillment of the requirements
for the degree of

Master of Science

in

Biomedical Engineering

TUFTS UNIVERSITY

Date

August 2017

Adviser:

Prof. Sergio Fantini, Ph.D.
Department of Biomedical Engineering, Tufts University

ABSTRACT

Coherent Hemodynamics Spectroscopy (CHS) is a novel technique based on quantitative relationships between cerebral hemodynamic oscillations and relevant physiological parameters like cerebral blood volume (CBV), cerebral blood flow (CBF), and metabolic rate of oxygen ($CMRO_2$). Protocols to induce oscillations in mean arterial blood pressure have been implemented for Coherent Hemodynamics Spectroscopy, to acquire cerebral hemodynamic oscillations at specific frequencies, employing techniques like Near-infrared Spectroscopy. The near-infrared window (700- 900 nm) of the electromagnetic spectrum is sensitive to the oxygenated and deoxygenated forms of hemoglobin, and allows for the measurement and quantification of their concentrations in tissue.

A crucial aspect for the optimal application of Coherent Hemodynamics Spectroscopy is the implementation of pertinent experimental protocols, with the focus being on eliciting *Coherent* cerebral hemodynamic oscillations. This is key for the optimal application of the quantitative relationships between cerebral physiological parameters and these induced oscillations. However, there exists an open question of whether the currently applied CHS protocols yield such significant hemodynamic oscillations.

In this thesis, modifications to the existing Coherent Hemodynamics Spectroscopy experimental protocols were implemented, to uncover optimal experimental conditions and measurement protocols that induced cerebral hemodynamic oscillations significant enough in terms of coherence, that is the oxy- and deoxy-

hemoglobin oscillations were optimally phase-locked with one another. The activation induced perturbation technique used here was based on the inflation and deflation of pneumatic thigh and arm cuffs.

The first portion of this study was devoted to deducing an optimal cuff occlusion pressure, which would then be implemented in future studies involving the cuff occlusion technique. The next portion dealt with determining optimal cuff positioning, which would induce maximal *Coherent* oscillations for CHS. Results of this study involved examining features of the oscillations suitable for CHS, like the Phase Synchronization Index (PSI). PSI quantifies the degree of phase-lock between the two signals considered and serves as a measure of coherence between them.

We found that a cuff inflation pressure of at least 160 mmHg is required to induce *Coherent* cerebral hemodynamic oscillations. Furthermore, in the study of arm and thigh cuffs, we established that the two thigh cuffs elicited highest *Coherent* hemodynamic oscillations. These results advance the development of pneumatic cuff based protocols for CHS, indicating optimal cuff locations and cuff inflation pressure.

ACKNOWLEDGEMENTS

I would firstly like to thank Dr. Sergio Fantini for having supervised my research. Without his guidance, and generously provided time and insight, completing this study would not have been possible. I am grateful to my fellow DOIT Lab members for allowing me to cope with the intricacies and background of the DOIT Lab research work, and for all the enjoyable times we shared as a team.

A special thank you to my family, whose support and unwavering optimism, helped me pursue an advanced degree in Biomedical Engineering.

Finally, thanks to my committee members, Dr. Irene Georgakoudi and Dr. Brian Tracey, for their time and consideration.

Table of Contents

LIST OF TABLES

LIST OF FIGURES

Chapter 1

Chapter 2

Chapter 3

Chapter 4

OPTIMIZATION OF PNEUMATIC-CUFF BASED PROTOCOLS FOR COHERENT HEMODYNAMICS SPECTROSCOPY

CHAPTER 1

NEAR-INFRARED SPECTROSCOPY AND COHERENT HEMODYNAMICS SPECTROSCOPY

1.1 NEAR INFRARED SPECTROSCOPY

1.1.1 Introduction

Near Infrared Spectroscopy (NIRS) is an optical technique that utilizes the near-infrared region of the electromagnetic spectrum for diagnostic and imaging studies of biological tissue. NIRS is sensitive to the oxygenated and deoxygenated forms of hemoglobin and focusses on the measurement as well as quantification of the tissue concentrations of these two forms. Medical application of NIRS is based on the concept that when near-infrared light is transmitted to and detected from human body tissues, it would hold hemoglobin concentration changes related information. For instance, when a particular region of the human brain is activated, continuous monitoring of blood hemoglobin levels through the determination of optical absorption of tissue is afforded by optical imaging.

1.1.2 Functional near infrared spectroscopy

The wavelength region from 700nm to 900nm, also referred to as the Near Infrared Window, is used to probe the cortical surface of the human brain in Functional Near Infrared Spectroscopy (fNIRS). The key tissue elements responsible for absorption in this window are oxy-hemoglobin (HbO_2) and deoxy-hemoglobin (Hb) (Fig. 1). A stimulus would induce changes in the intensity of detected optical signal due to local variations of oxy- and deoxy-hemoglobin concentrations. The modified Beer-Lambert law (mBLL) can be applied to relate these optical intensity changes to concentration changes of hemoglobin.

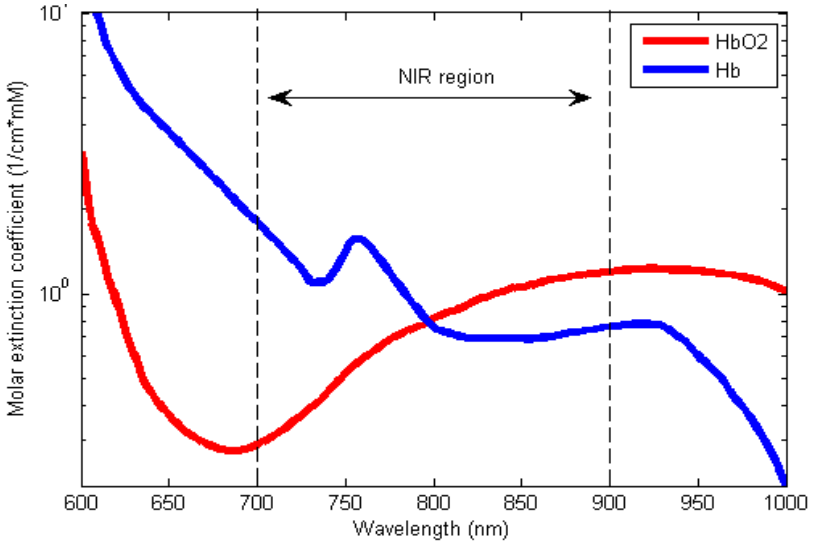

Figure 1. Absorption Spectra of Hemoglobin

Curtin, Adrian.” Functional Near Infrared Spectroscopy.” Wikipedia. Web.

Being a non-invasive technique that has high temporal resolution (up to a few tenths of ms), good spatial resolution (about 5 mm) and cost-effectiveness, fNIRS is now finding increasing applications in brain studies. (Sassaroli et al. 2008)

The instrumentation involves laser diodes emitting near infrared light using fiber optics located on the head. These fibers are kept in place by headgears supporting the pattern of source-detector fibers used. The portion of the optical intensity that leaves the tissue due to scattering events which depend on tissue optical properties is then collected by the detector fibers and carried to the data processing unit.

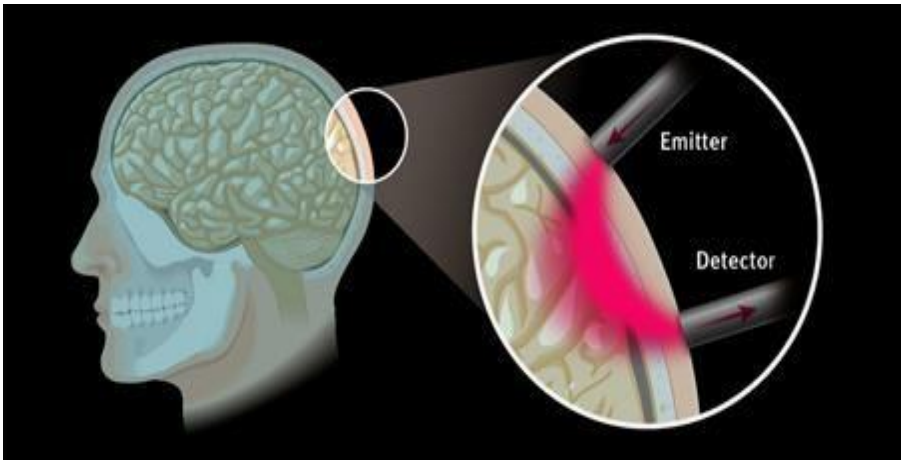

Figure 2. Near Infrared light transmission through human brain tissue using Imagent™ (the tissue spectrometer).

"Imagent™." www.iss.com. ISS, Inc., Web.

1.2 COHERENT HEMODYNAMICS SPECTROSCOPY

1.2.1 Blood vasculature

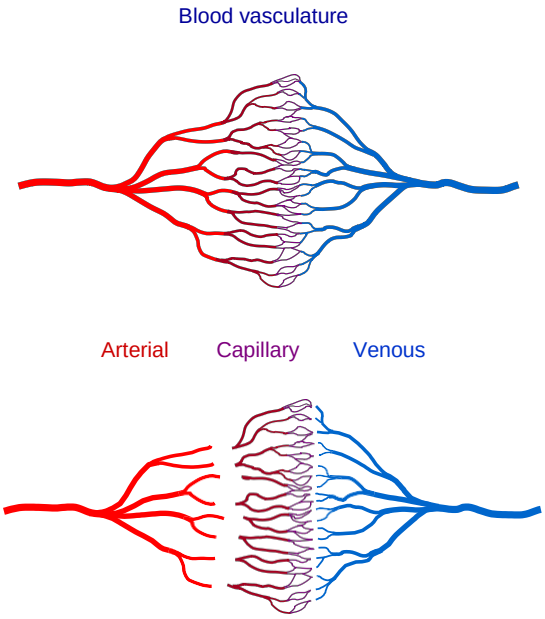

Figure 3. Blood vasculature comprising of arterial, capillary, and venous components.
Cassot, Francis, Frederic Lauwers, Céline Fouard, Steffen Prohaska, and Valerie Lauwers-Cances. "A novel three-dimensional computer-assisted method for a quantitative study of microvascular networks of the human cerebral cortex." *Microcirc* 13 (2006):1-18. Web.

The blood vasculature is comprised of three main blood compartments, arterial, capillary and venous, as shown in Fig. 3.

The arterial portion of the vasculature includes arteries and arterioles. Arteries perform the function of carrying highly oxygenated blood away from the heart to different bodily tissues. Arterioles are the narrower version of arteries that branch off into and carry blood to the capillaries.

Capillaries being the smallest and thinnest of the blood vessels are more frequently found. They connect to the arterial portion on one end and the venous on the other.

Capillaries are responsible for facilitating gaseous, nutrients, and waste products exchange between blood vessels and tissues. The endothelium that lines the capillaries performs as a filter, trapping the blood cells inside of the vessels while allowing diffusion of essential elements facilitated by a concentration gradient.

Venules connect capillaries to veins, thus carrying deoxygenated blood away from capillaries into larger blood vessels, veins. Veins return this deoxygenated blood to the heart.

Therefore, oxygen delivery to tissues occurs through transfer of oxygen from hemoglobin in the vasculature into plasma, and transmission facilitated by a concentration gradient from plasma to tissue. (Fantini. 2014)

1.2.2 Hemodynamic oscillations and CHS

Time-dependent changes in cerebral oxy- and deoxy- hemoglobin concentrations can be attributed to changes in cerebral blood volume (CBV), cerebral blood flow (CBF), and metabolic rate of oxygen ($CMRO_2$). (Kainerstrofer, Sassaroli, and Fantini. 2014). Protocols to induce oscillations in mean arterial blood pressure have been adopted and implemented for Coherent Hemodynamics Spectroscopy to acquire cerebral hemodynamic oscillations at specific frequencies, employing methods like optical imaging and fNIRS. It has been presented that the CHS model can be applied to obtain the phase and amplitude of those induced hemodynamic oscillations, thereby allowing the deriving of physiologically relevant parameters. (Fantini. 2014)

Specifically, this model can assess the consequence of activation-induced perturbations in cerebral blood flow, cerebral blood volume and local oxygen consumption.

1.2.3 Measures of suitability factors for CHS

The features of measured hemodynamic oscillations suitable for CHS are,

1. Phase Synchronization Index (PSI)

   Phase synchronization occurs when two or more periodic signals oscillate with stable comparative phase angles. In this study, PSI was used to quantify the degree of phase-lock between the measured optical intensity signals collected at 690 and 830 nm for duration of the perturbation-induced activation protocol. The phase-lock between extracted Oxy- and Deoxy-hemodynamic oscillations was also calculated using the PSI. First, the time dependent phase difference (ϕ) between the signals was computed using the Hilbert Transform (Pierro et al., 2012), followed by derivation of PSI for each induced oscillation segment.

$$PSI = 1 - \frac{S}{\ln(N)} \qquad (1)$$

   Where, $S = -\sum_{i=1}^{N} P(i)(\ln P(i))$

   Here, N=72, is the number of bins between 0 to 2π. Here $P(i) = \frac{n(i)}{\sum_{i=1}^{N} n(i)}$

   i enumerates the the bins in which the 0 - 2 π range is divided, and n(i) is the number of phase observations in bin i.

Signals that do not have a constant phase difference would yield a PSI=0, and a PSI=1 would mean that the signals are perfectly synchronized referring to a constant phase-lock. (Wigal et al. 2012)

2. Statistical test for relative phase

   P value is the probability of obtaining the observed result (or more extreme) assuming that the null hypothesis is true. The null hypothesis being the condition of no phase synchronization between the two optical intensity signals (at 690 and 830 nm) or, the oxy and deoxy hemodynamic oscillations. The p value ranges from 0 to 1 and the smaller the p value the greater the probability that the observed result does not follow the null hypothesis. For this study, the hypothesis testing was executed by generating a null statistic. The alternative hypothesis being the existence of a constant phase difference (phase-lock) between the optical intensity data (at 690 and 830 nm) or, the oxy and deoxy hemodynamic oscillations, was tested against the null hypothesis and a 5 % level of significance (α), was considered to conclude the suitability of measured results for CHS (calculation explained in detail in Chapter 3).

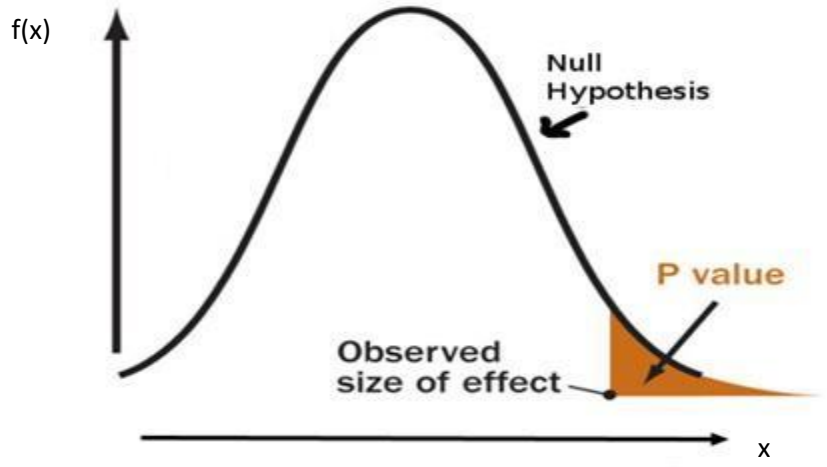

Figure 4. The p value is represented by the shaded area and a 5 % level of significance was implemented. The x axis represents a continuous random variable x, and the y axis shows its probability density function, f(x).

1.2.4 CHS VS NIRS

As we know, NIRS allows for the measurement of oxy- and deoxy-hemoglobin concentration changes. Quantifying the contributions of physiological processes towards measured signals using NIRS, is where the applicability of CHS comes in. Being a mathematical model implemented for signal interpretation, important cerebral physiological parameters, for instance the capillary transit time (t_c), can be measured during different physiological/pathological states of the human brain using CHS. To summarize, CHS can be used to measure cerebral parameters like cerebral autoregulation, cerebral blood flow (CBF), and possibly the metabolic rate of oxygen consumption (CMRO2), which cannot be measured by NIRS alone.

CHAPTER 2

EXPERIMENTAL PROTOCOLS FOR COHERENT HEMODYNAMICS SPECTROSCOPY

CURRENTLY APPLIED PROTOCOLS FOR COHERENT HEMODYNAMICS SPECTROSCOPY

Coherent Hemodynamics Spectroscopy utilizes induced cerebral hemodynamic oscillations measured at multiple frequencies using near-infrared spectroscopy to analyze and obtain physiologically relevant information. The currently applied protocols to induce cerebral hemodynamic oscillations at specific frequencies include paced breathing (Reinhard et al. 2006; Pierro et al. 2014) and pneumatic thigh-cuff inflation, including both the one thigh (Pierro et al. 2014) and two thighs occlusion techniques. (Kainerstorfer et al. 2015).

In all protocols described in subsequent sections of this chapter, near-infrared spectroscopy measurements were obtained using a commercial tissue oximeter (OxiplexTS, ISS, Inc., Champaign, IL). The delivery of light at two wavelengths, 690 and 830 nm and collection were performed using optical probes, composed of two illumination fibers (for the two incident wavelengths) and one collection fiber bundle. The probe was placed either on the left or right side of the subject's forehead and secured with a flexible black headband to ensure no interference from room light. A 3.5 cm illumination source- collection detector separation was used and the detection sampling rate was 6.25 Hz.

For the pneumatic thigh cuffs protocol, inflation-deflation of the cuff was facilitated by an automated cuff inflation device (E-20 Rapid Cuff Inflation System, D. E. Hokanson, Inc., Bellevue, Washington).

Modified Beer-Lambert Law (Delpyet al., 1988; Sassaroli, and Fantini. 2004) was implemented to extract Oxy- and Deoxy- hemoglobin time traces from optical intensities measured employing these protocols (in-depth explanation in Chapter 3).

Written informed consent was obtained prior to each study from all participants.

2.1 PACED BREATHING (Pierro et al. 2014)

The protocol required the subject to be in a seated position and used a breathing metronome (shown in Fig. 4), the "Paced Breathing" Android™ application as a visual guide. Paced breathing was thus performed at specific frequencies between 0.07-0.25 Hz. The procedure involved an initial 30 s baseline measurement, succeeded by eleven 120s paced breathing cycles (one for each frequency) interrupted by 60 s of spontaneous breathing sections. Simultaneous recording of respiration data was done by placing a strain gauge (Ambu Sleepmate Piezo Effort Sensor), around the subject's chest and an auxiliary input port of the tissue spectrometer received its output. The entire set-up is show in Fig. 5.

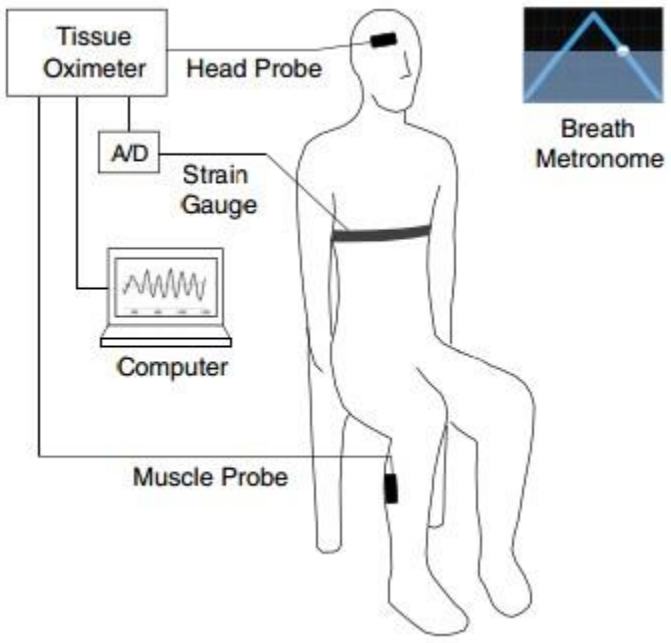

Figure 5. Schematic diagram of experimental set-up.

Pierro, Michele L., Bertan Hallacoglu, Angelo Sassaroli, Jana M. Kainerstrifer, and Sergio Fantini. "Validation of a novel hemodynamic model for coherent hemodynamics spectroscopy (CHS) and fuctional brain studies with fNIRS and fMRI." *NeuroImage* 85 (2014): 222-33. Web.

2.2 PNEUMATIC THIGH CUFF INFLATION

2.2.1 One thigh occlusion protocol (Pierro et al. 2014)

This study was performed on five hemodialysis patients, during the hemodialysis procedure, as well as six healthy subjects. Cerebral hemodynamic oscillations were induced using a pneumatic cuff placed around each subject's left thigh. The experimental set-up is shown in Fig. 6.

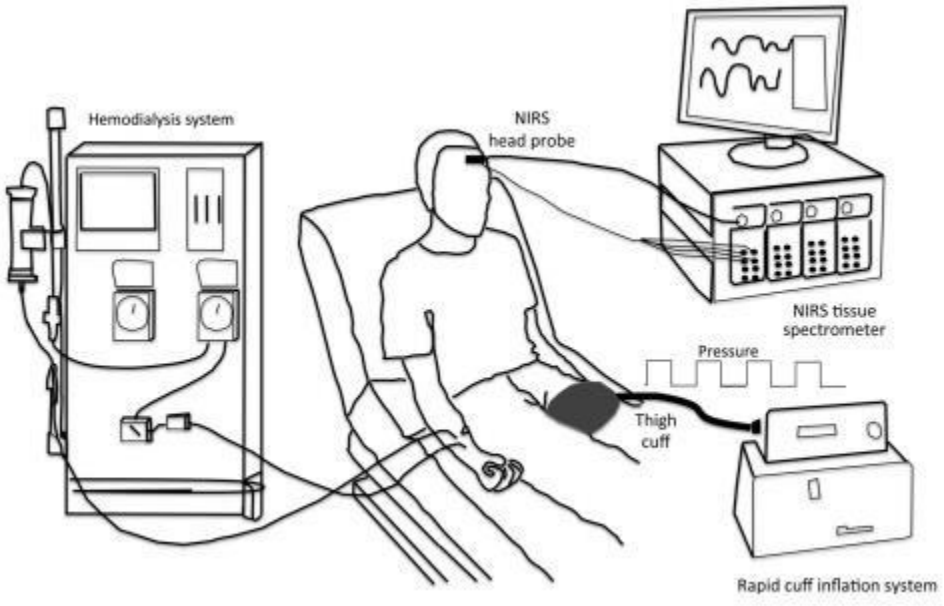

Figure 6. Schematic diagram of the experiment set-up for one thigh occlusion protocol for CHS. The same set-up was used for healthy subject's sans the hemodialysis system unit.

Pierro, Michele L., Jana M. Kainerstorfer, Amanda Civiletto, Daniel E. Weiner, Angelo Sassaroli, Bertan Hallacoglu, and Sergio Fantini. "Reduced speed of microvascular blood flow in hemodialysis patients versus healthy control: a coherent hemodynamics spectroscopy study." *Journal of Biomedical Optics* 19 (2014): 026005-1-026005-9. Web.

The inflation pressure was set at 200 mmHg. Seven frequencies between 0.03 to 0.17 Hz were induced, each induced for four periods with an interval of 1 minute to allow for subject recovery.

2.2.2 Two thigh occlusion protocol (Kainerstorfer et al. 2015)

The mean arterial pressure (MAP) was recorded using a beat-to-beat finger plethysmography system (NIBP100D, BIOPAC Systems, Goleta, CA, USA). Thigh cuffs were placed around each thigh and inflated-deflated to a pressure of 200 mmHg. A respiration belt around the chest monitored respiration. The experimental set-up is shown in Fig. 7.

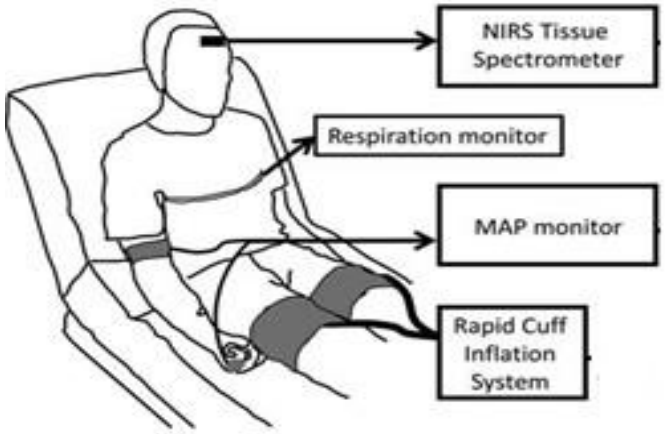

Figure 7. Schematic diagram of two thigh occlusion experiment protocol.

Kainerstorfer, Jana M., Angelo Sassaroli, Kristen T. Tgavalekos, and Sergio Fantini. "Cerebral autoregulation in the microvasculature measured." *Journal of Cerebral Blood Flow & Metabolism* 35 (2015): 959-66. Web.

The protocol procedure comprised of 2 minutes' baseline measurements followed by the thigh cuffs inflation at 200 mmHg for 2 minutes. After two minutes of cuff deflation, they were inflated again at 200 mmHg and the subject was asked to hyperventilate simultaneously for 2.5 minutes.

The cuff perturbation technique induced changes in MAP, which resulted in changes in cerebral Oxy, De-oxy and Total hemoglobin.

CHAPTER 3

OPTIMIZATION OF PROTOCOLS FOR COHERENT HEMODYNAMICS SPECTROSCOPY

3.1 OPEN QUESTIONS TO CURRENTLY APPLIED CHS EXPERIMENTAL PROTOCOLS

A principal factor in fNIRS studies is the application of pertinent protocols for brain activation. (Sassaroli et al. 2008). For Coherence Hemodynamics Spectroscopy, the high coherence factor of induced cerebral hemodynamic oscillations coupled with the ability to elicit such oscillations at desired frequencies, is the key to optimal quantification of the relationship between physiological parameters and induced cerebral hemodynamic oscillations, collected using NIRS. This objective was sought to be achieved with the currently applied CHS protocols.

However, there exists an open question (Pierro et al., 2014; Pierro et al., 2014) of whether the currently applied CHS protocols yielded induced oscillations that were significant enough in terms of coherence and amplitude, that is if the optical intensities (690 and 830 nm) and/or the extracted oxy- and deoxy- hemoglobin time traces were optimally phase-locked with one another and possessed a significant phase relation with the activation induced perturbation.

The purpose of this study was to uncover and implement modifications to the existing CHS experimental protocols, to ensure optimal measurement of induced *coherent* cerebral hemodynamic oscillations. This understandably forms a crucial aspect as it defines the *Coherence* in Coherence Hemodynamics Spectroscopy, thereby making it an important pre-requisite in data that is analyzed by the model.

As described in the cuff occlusion protocol section of this chapter, the thigh cuff occlusion pressure implemented was at 200 mmHg. It is unclear as to whether previous studies were conducted by our group, to form the basis for the use of this occlusion pressure value. The first part of this study involved concluding an optimal cuff occlusion pressure value which would form the foundation for future studies implementing the cuff occlusion protocol. The two-thigh occlusion protocol previously explained was applied at pressure values ranging from 80 to 200 mmHg in steps of 20 mmHg, each occlusion period lasting for 72 seconds with a minute of resting period inserted between successive occlusion periods. The frequency of oscillations here was 0.0833 Hz and was chosen keeping the length of the protocol in mind.

The next portion of this study comprised of obtaining induced cerebral hemodynamic oscillations measured using various cuff combinations and positions including two arms, two thighs, one arm and one thigh, at the occlusion pressure value concluded from the first part of this study. The goal here was to uncover a cuff occlusion protocol in terms of cuff positioning, which would elicit maximal 'coherent' induced cerebral hemodynamic oscillations for CHS. Frequency of oscillations was 0.0833 Hz.

Features of collected induced hemodynamic oscillations used to deduce significance of the measurements obtained from this study, as described in Chapter 1 are,

1. Phase synchronization index
2. A statistical test (p value) to check the significance of obtained results

3.2 TWO-THIGH OCCLUSION PROTOCOL FOR A RANGE OF PRESSURES

The goal here was to determine the pressure at which the two-thigh cuff occlusion led to most significant changes in the subject's MAP, thereby inducing changes in cerebral oxy-, deoxy-, and total hemoglobin measured and collected by the tissue spectrometer.

Written informed consent was obtained from subjects prior to the study. The subjects had no history of neurologic diseases, or cardiovascular diseases. The two-thigh occlusion protocol previously implemented by our group, was performed at seven different inflation pressure values, 80, 100, 120, 140, 160, 180, and 200 mmHg. The two pneumatic thigh cuffs were placed around both thighs of the subject and connected to an automated cuff inflation system. (E-20 Rapid Cuff Inflation System, D. E. Hokanson, Bellevue, WA, USA) whose adjustable pressure crank allowed for varying pressures, ranging from 80 to 200 mmHg, with increments applied in steps of 20 mmHg.

The occlusion period lasted for 72 s for each pressure value and consisted of 6 cuff inflation-deflation cycles, each lasting for 12 seconds (6 seconds of cuff inflation followed by 6 seconds of deflation). The protocol consisted of 2 minutes of baseline measurements initially, after which the cuffs were inflated at the 7 different pressures (80, 100, 120, 140, 160, 180, and 200 mmHg), with a 60 s of resting interval inserted between successive occlusion periods, during which the cuffs remain deflated, as shown in Fig. 8b.

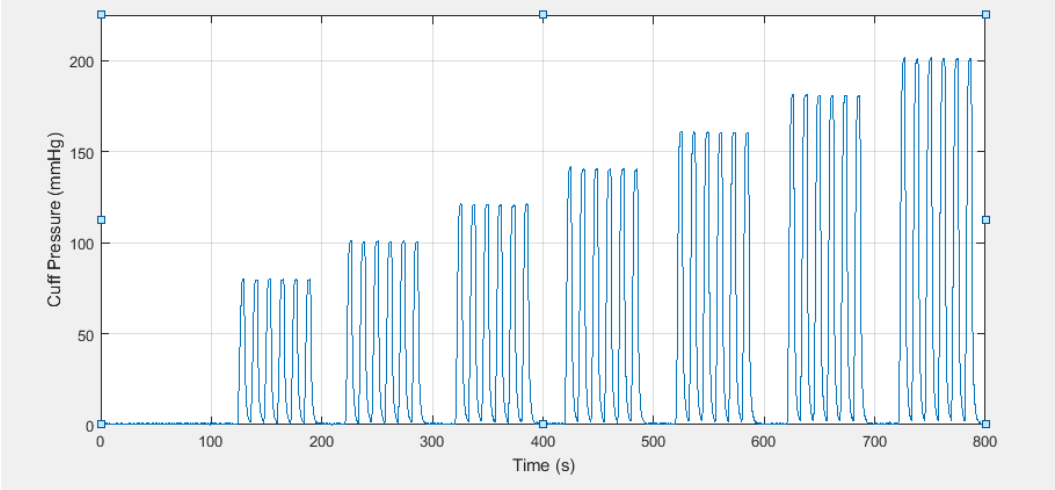

a.

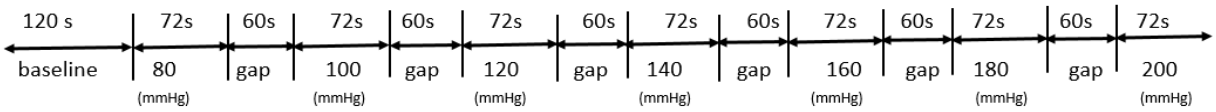

b.

Figure 8 a. Representation of two thigh cuff occlusion protocol implemented at a range of pressures starting at 80 mmHg up to 200mmHg, with increments in steps of 20 mmHg. (80, 100, 120, 140, 160, 180, and 200 mmHg).
b. Sequence of the protocol with an occlusion period lasting for 72 seconds and each cuff oscillation for 12 seconds. A resting interval of 60s was included in between successive occlusion periods.

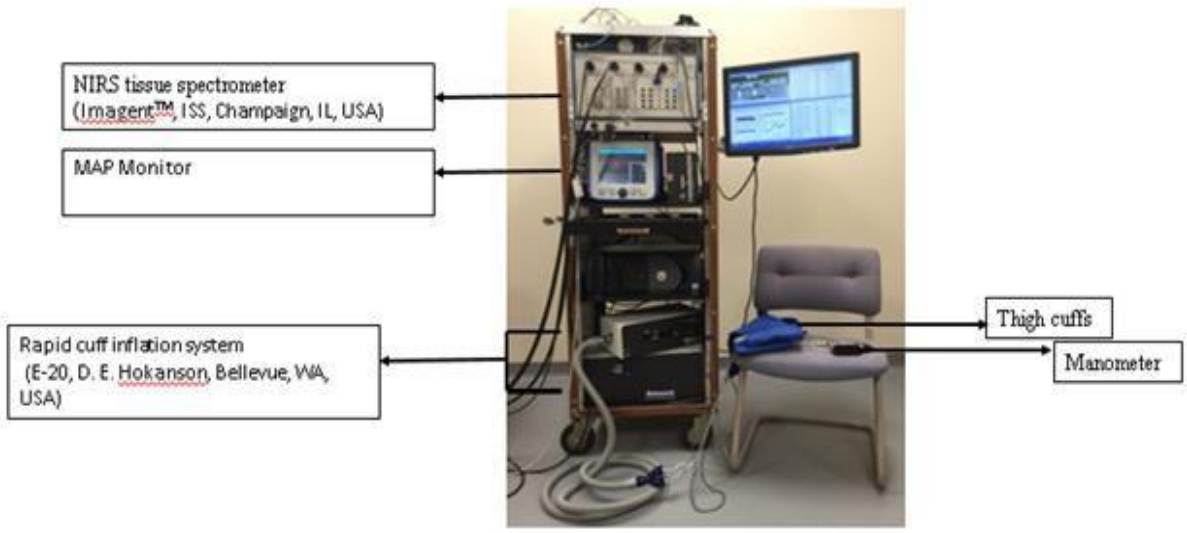

Figure 9. Components involved in the acquisition of induced cerebral hemodynamic oscillations using NIRS.

The rapid inflation of the two thigh cuffs resulted in variation of the mean arterial pressure, which was continuously monitored using the MAP monitor and beat-to-beat finger plethysmography system (NIBP100D, BIOPAC Systems, Goleta, CA, USA). Data from all these systems was sent to an auxiliary input module (ISS, Champaign, IL, USA) followed by a computer where it was consolidated to make it suitable for MATLAB processing. A tissue spectrometer (Imagent™, ISS, Champaign, IL, USA) operating at 690 and 830 nm was used for collection of NIRS data.

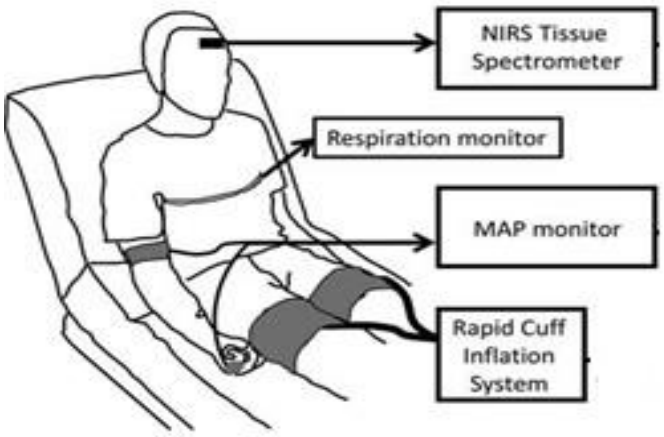

Figure 10. Schematic of experiment set-up. The pneumatic thigh cuffs are placed around the subject's thighs and inflated by the rapid cuff inflation system. The NIRS spectrometer collects the hemodynamic oscillation traces. MAP and respiration are continuously monitored.

Kainerstorfer, Jana M., Angelo Sassaroli, Kristen T. Tgavalekos, and Sergio Fantini. "Cerebral autoregulation in the microvasculature measured." *Journal of Cerebral Blood Flow & Metabolism* 35 (2015): 959-66. Web.

Fig. 10 details the set-up for data collection. An optical probe was placed on the right portion of the subject's forehead and secured using a black headband, which also aims to prevent interference from room light. The probe was composed of two illumination fibers (one for each of the two incident wavelengths, 690 and 830 nm) and one collection fiber bundle. A 3.5 cm illumination source- collection detector separation was used and the sampling rate was 6.25 Hz.

3.3 VARIED CUFF POSITIONS WITH INFLATION AT THE OPTIMAL PRESSURE

The purpose of this next study was to determine the cuff occlusion position(s) which elicited the most *Coherent* induced cerebral hemodynamic oscillations.

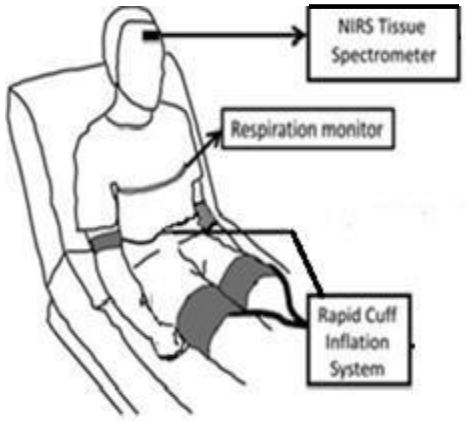

Figure 11. The experiment set-up used for data acquisition.

The varied positions cuff occlusion protocol utilizes the same components described in Fig. 8, with a slight modification in the set-up. The only addition are two arm cuffs that were applied around both arms of the subject. Due to the placement of the arm cuffs on both arms, continuous monitoring of MAP was not an available option.

Healthy female subjects (age range: 23-28), with no history of neurological or cardiovascular diseases participated in the experiment. Written informed consent was obtained prior to the study.

Four cuffs, two thigh cuffs and two arms cuffs were used, and a two Y connector tube was used to connect the four cuffs to the cuff inflation system. (E-20 Rapid Cuff Inflation System, D. E. Hokanson, Bellevue, WA, USA). The cuffs were inflated at 180 mmHg, the pressure value deduced from the study of the two-thigh occlusion protocol for a range of pressures. This deduction is explained in detail in the following chapter, which documents the results obtained.

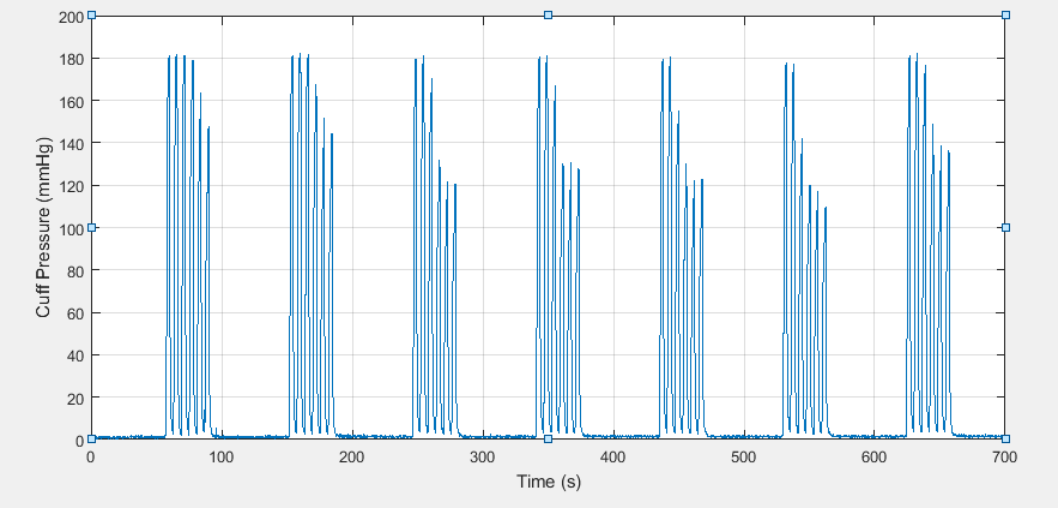

Figure 12. Diagram representing the varied cuff occlusion positions protocol implemented at 180 mmHg. The sequence includes first the right thigh (RT), followed by the left thigh(LT), right arm(RA), left arm(LA), two thighs(2T) and, two arms(2A).

The protocol involved an initial two-minute baseline measurement, followed by the different cuff occlusion positions. Each occlusion duration was 72 seconds, consisting of 6 cuff inflation-deflation cycles lasting for 12 seconds each that is 6 seconds of cuff inflation followed by 6 seconds of deflation, at a frequency of 0.0833 Hz. The sequence of cuff occlusion positions started with first the right thigh (RT), followed by the left thigh (LT), right arm (RA), left arm (LA), two thighs (2T) and two arms (2A).

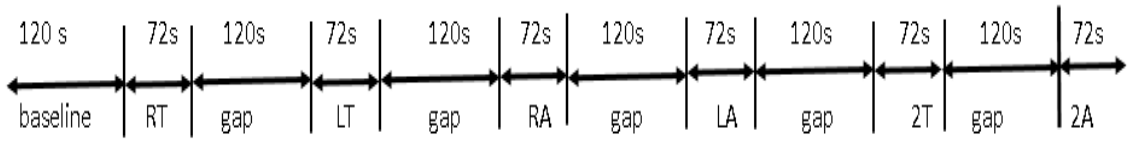

Figure 13. Representation of the sequence of cuff occlusions at varied positions. Each occlusion lasts for 72 seconds and includes the right thigh (RT), followed by the left thigh (LT), right arm (RA), left arm (LA), two thighs(2T), and two arms(2A).

With the help of the optical probe placed on the subject's forehead, changes in the optical intensities over time were measured by the tissue spectrometer.

(Imagent^{TM}, ISS, Champaign, IL, USA).

3.4 DATA ANALYSIS

3.4.1 Two-thigh occlusion protocol for a range of pressures

The optical intensities data (at 690 and 830 nm) collected through NIRS at a sampling rate of 6.25 Hz and a source-detector separation of 35 mm, was subjected to third order polynomial detrending, to account for any slow temporal drifts.

The detrended optical intensities and MAP (mean arterial pressure) time traces were then band-pass filtered using a linear-phase bandpass filter (function 'firpmord' in MATLAB, MathWorks, Natick, MA, USA), based on the Parks-McClellan algorithm (Parks, and McClellan. 1972). The center frequency of this filter (f_0) was assigned to be the thigh cuff inflation-deflation frequency, in this case, 0.0833 Hz. The bandwidth of the band-pass filter was set to $f_0 \pm 0.025$ Hz. A smaller bandwidth was implemented to ensure that the analysis was performed on oscillations measured and induced at the thigh cuff inflation-deflation frequency (0.0833 Hz). The cyclic pressure was applied for 72 s, which would relate to an intrinsic bandwidth of $\frac{1}{72\ s} = 0.014$ Hz. Therefore, a bandwidth of ± 0.025 Hz was chosen for data analysis.

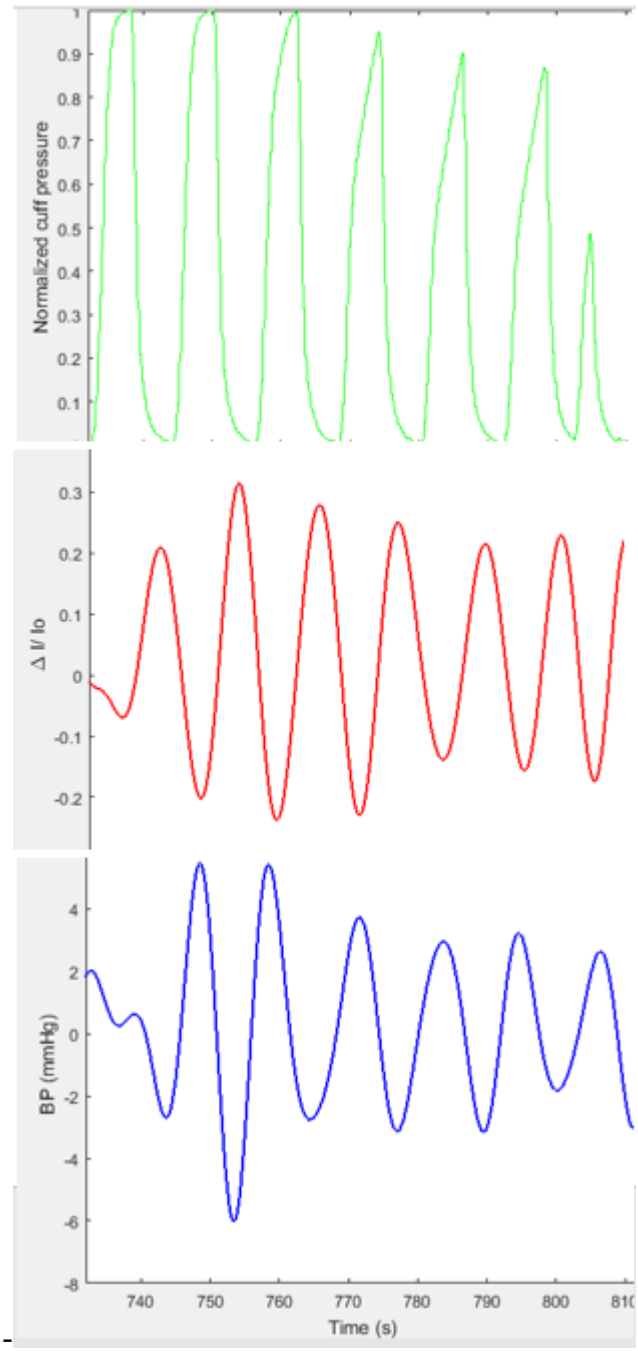

Figure 14. Typical example of a measured time trace over one occlusion period, band-pass filtered at $f_0 \pm 0.025$ Hz. (Data from subject 2). The top panel illustrates the cuff pressure. The center panel demonstrates the band-pass filtered time trace of the optical intensity at 830nm. The lower panel is the MAP (mean arterial pressure) time trace.

The instantaneous phase difference between the optical intensitytime traces at 690 and 830 nm were computed by subtracting the instantaneous phases of the data at 830 nm from the data at 690 nm. The instantaneous phases of data at both 830 nm and 690 nm were obtained by the analytic signal method.

$$a(t) = x(t) + jx\tilde{}(t) = M(t)e^{j\Phi(t)} \quad (2)$$

$$x\tilde{}(t) = \frac{1}{\pi} p.v. \int_{-\infty}^{\infty} \left[\frac{x(t')}{(t - t')} \right] dt' \quad (3)$$

The analytic signal, $a(t)$, is a complex extension of a real signal $x(t)$ where the imaginary part is given by the Hilbert Transform of the real signal, $x\tilde{}(t)$ (Gabor 1946)(Pierro et al., 2012). *M(t)* is the instantaneous amplitude of the analytic signal (also known as the envelope of the real signal s(t)), Φ(t) is its instantaneous phase, and p.v. denotes the Cauchy principal value. (Byun et al., 2016; Kainerstorfer, Sassaroli, and Fantini. 2014)

Once this phase difference between the 830 and 690 nm data were obtained at time intervals defined by the duration of each occlusion period, the degree of phase-lock between the two intensity traces was quantified by the phase synchronization index (PSI) shown previously in Eq. 1. It calculates the average phase difference between the two signals over the entire run.

The algorithm considers the data points over a defined interval of time. In this case, that would be the duration of the occlusion period. Each time interval is divided into N = 72 bins and the probability of the distribution of phase synchronization between the 830 and 690 nm signals is computed. The phases are then averaged over all N bins thereby determining the phase synchronization index.

To check the significance of the calculated PSI values of each experiment, a null statistic was generated from collected phantom data, that represented a probability density function of PSI value occurrences (ranging between 0 and 1), under the conditions of no phase synchronization between the two optical intensity signals (at 690 and 830 nm). To generate this statistic, data analyses conditions of experimentally collected data were replicated. The algorithm was implemented on phantom data (i.e measurements obtained from phantoms) for the exact same time-interval data points and sample size as the obtained measurements. Identical filter characteristics and sampling rate were assigned to this phantom data. Identical to the method explained previously, Hilbert transform was then used to compute the instantaneous phase of filtered phantom data, followed by calculation of the phase synchronization index.

The calculation of PSI was repeated for 10000, to generate a histogram that represented the probability of occurrence of PSI values on the y axis and PSI values on the x- axis. A 0.05 level of significance was considered to check the significance of observed experimental results and to negate the null hypothesis.

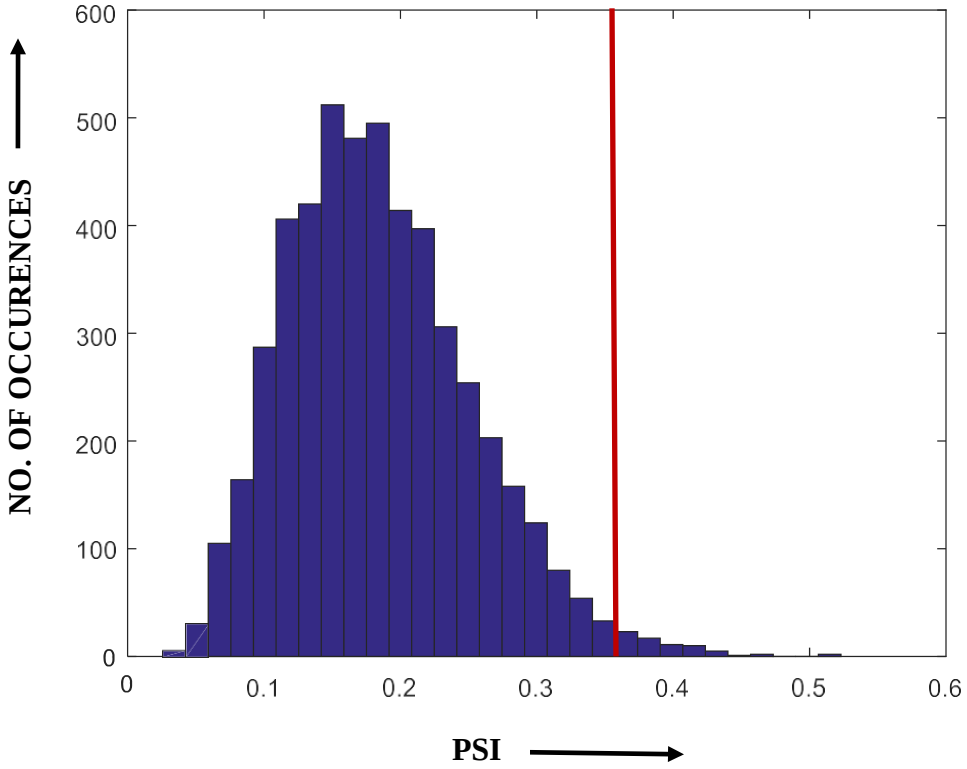

Figure 15. Typical example of the histogram generated by the null statistic algorithm. The y-axis depicts the probability of PSI value occurrence against the PSI values on the x-axis. A 5 % level of significance corresponds to a critical PSI value of 0.36, as indicated by the red line.

In the case of measured cerebral optical intensity signals (at 690 and 830 nm), a PSI greater than 0.36 would have a 5 % chance of occurring under the conditions of no phase synchronization between the signals.

3.4.2 Varied cuff occlusion positions protocol at the concluded pressure value

Data measured at each wavelength (690 and 830 nm), at a sampling rate of 6.25 Hz, was used to extract absorption changes in oxy- and deoxy- hemoglobin by applying the modified Beer-Lambert law (mBLL) (Delpy et al., 1988; Sassaroli and Fantini, 2004).

The modified Beer-Lambert Law:

The mBLL is commonly used in NIRS of highly scattering media to derive changes in optical absorption from measured changes in optical intensity. The idea is to relate differential intensity measurements to differential measurements of tissue absorption. Here, the term differential refers to measurements relative to a baseline, or initial state. The mBLL takes tissue scattering into account by considering the mean path length traveled by photons in tissue from the illumination to the optical collection point (Delpy et al., 1988). The differential path length factor (DPF) is defined as the ratio between such mean optical path length and the geometrical distance between illumination and collection points. In this work, we used DPF values of 6.51 at 690 nm and 5.91 at 830 nm to compute the tissue absorption coefficients at 690 and 830 nm, μa1 and μa2, respectively. Concentration changes in oxy- and deoxy hemoglobin was then obtained using the following equations,

$$\Delta O = \frac{(\Delta\mu a1 * \varepsilon_{d2}) - (\Delta\mu a2 * \varepsilon_{d1})}{(\varepsilon_{O1} * \varepsilon_{d2}) - (\varepsilon_{O2} * \varepsilon_{d1})} \quad (4)$$

$$\Delta D = \frac{(\Delta\mu a2 * \varepsilon_{O1}) - (\Delta\mu a1 * \varepsilon_{O2})}{(\varepsilon_{O1} * \varepsilon_{d2}) - (\varepsilon_{O2} * \varepsilon_{d1})} \quad (5)$$

Here, μ_{a1} and μ_{a2} are the absorption co-efficient of data at 690 and 830 nm respectively. ε_{O1} and ε_{O2} are the extinction co-efficients of oxy- hemoglobin at 690 and 830 nm, while ε_{d1} and ε_{d2} are the extinction co-efficients of deoxy-hemoglobin at 690 and 830 nm.

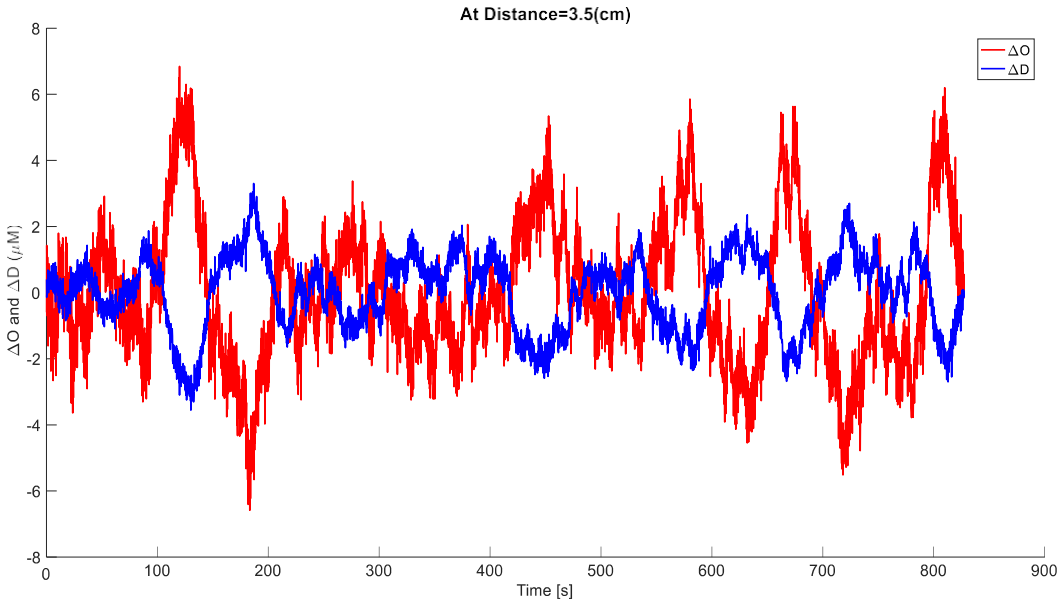

Figure 16. Typical example of extracted oxy- and deoxy- hemoglobin time traces obtained by applying the modified Beer-Lambert Law (data from subject 1).

Slow temporal drifts were removed using third order polynomial detrending. Following the calculation of O(t) and D(t) traces from the optical intensities, the algorithm followed a course similar to the data analyses implemented on the two-thigh occlusion protocol for a range of pressures. Linear band-pass filtering based on the Parks –McClellan algorithm, was applied to the O(t) and D(t) traces at a center frequency f_0 = 0.0833 Hz, using a bandwidth $f_0 \pm$ 0.025 Hz. The instantaneous phase of the oxy- and deoxy- hemoglobin time traces was computed using the Hilbert Transform as described previously (function 'hilbert' in MATLAB, MathWorks, Natick, MA, USA). The instantaneous phase difference between the two signals was computed at time intervals defined by the duration of each occlusion period, followed by the computation of their phase synchronization index using Eq. 1.

The significance of the results obtained using this protocol was verified by developing a null statistic like the method used in the two-thigh occlusion protocol for a range of pressures. In this case, extracted oxy- and deoxy- hemoglobin time traces were considered, and a 5% level of confidence corresponded to a PSI critical value of 0.6.

CHAPTER 4

RESULTS AND FUTURE SCOPE

This chapter entails the presentation of results obtained using the two-thigh occlusion protocol for a range of pressures and the varied cuff-occlusion positions protocol, along with the discussion and implication of these results. A look into the future scope of experiment protocols for Coherent Hemodynamics Spectroscopy has also been explored.

4.1 TWO-THIGH OCCLUSION PROTOCOL FOR A RANGE OF PRESSURES

The experimental protocol lasted for 17 minutes and the measured, band-pass filtered cerebral optical intensity time series at 830 nm is as shown in Fig. 17 a, simultaneously with the cuff oscillations at 0.0833 Hz. The measured mean arterial blood pressure time series synchronous with the cuff oscillations is shown in Fig. 17 b. The average measured MAP for subject 1 was found to be 105 mmHg.

Fig. 18 provides a zoomed in view of the measured and filtered oscillations at 830 nm, at each of the seven pressure occlusion periods, 80, 100, 120, 140, 160,180, and 200 mmHg for subject 1.

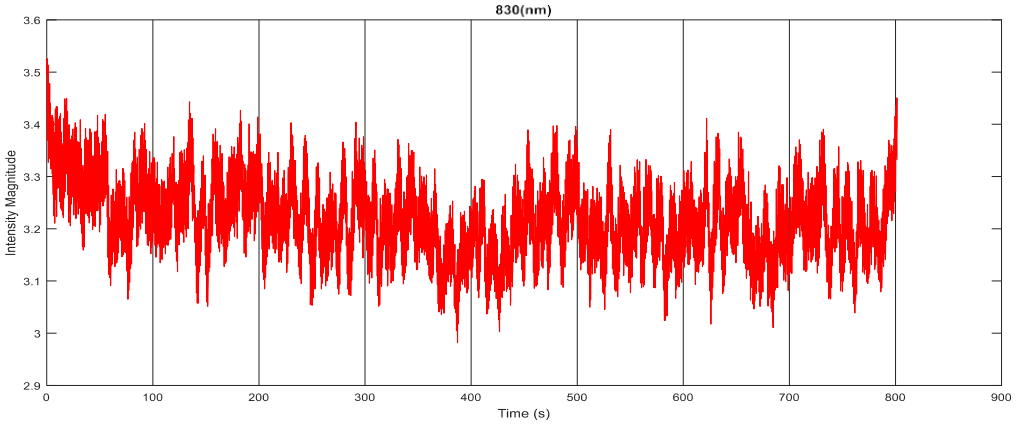

a.

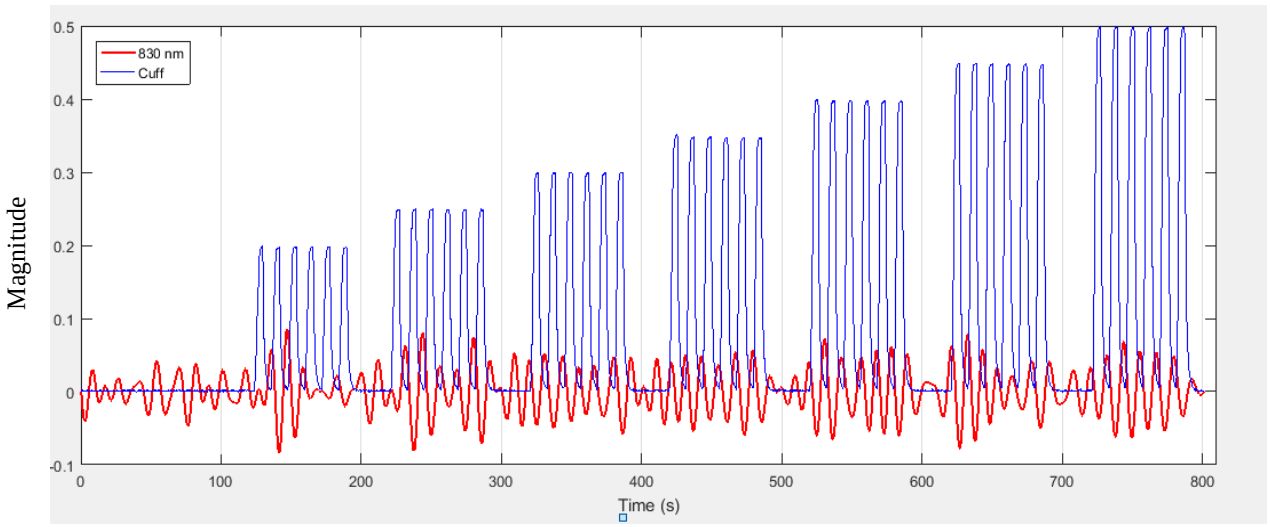

b.

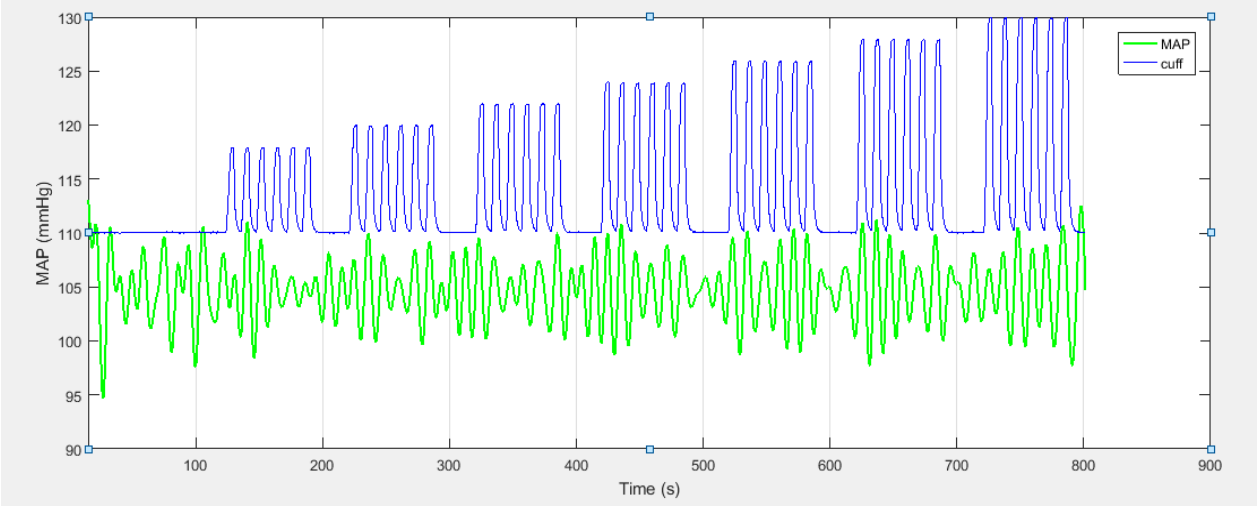

c.

Figure 17 a. Raw time trace of the optical intensity signals obtained at 830 nm. b. Band-pass filtered cerebral optical intensity time trace measured at 830 nm shown simultaneously along with the cuff oscillations. c. Measured and band-pass filtered mean arterial blood pressure(MAP) time trace simultaneous to the cuff oscillations. Both traces were measured from subject 1.

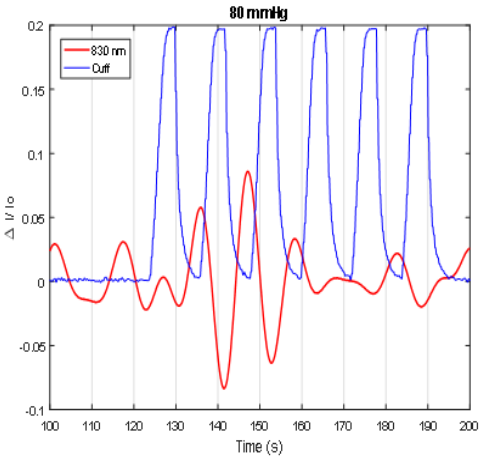
80 mmHg
830 nm
Cuff
Δ I/ Io
Time (s)

a

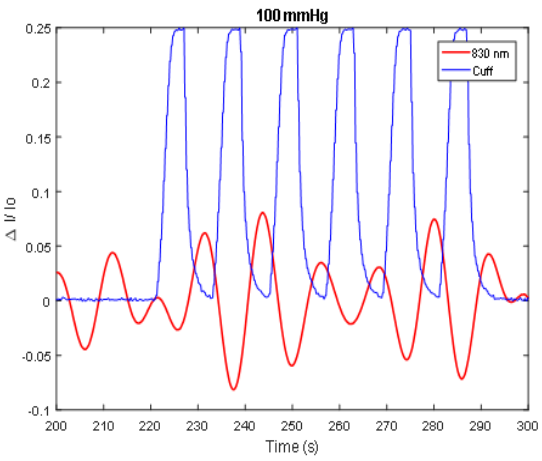
100 mmHg
830 nm
Cuff
Δ I/ Io
Time (s)

b

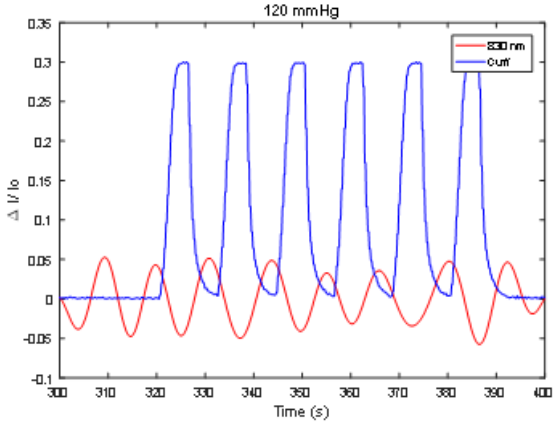
120 mmHg
830 nm
Cuff
Δ I/ Io
Time (s)

c

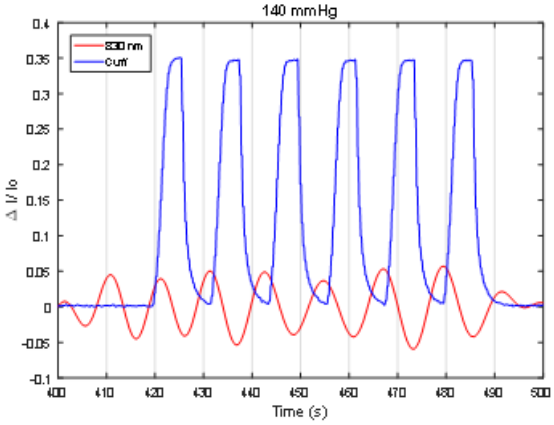
140 mmHg
830 nm
Cuff
Δ I/ Io
Time (s)

d

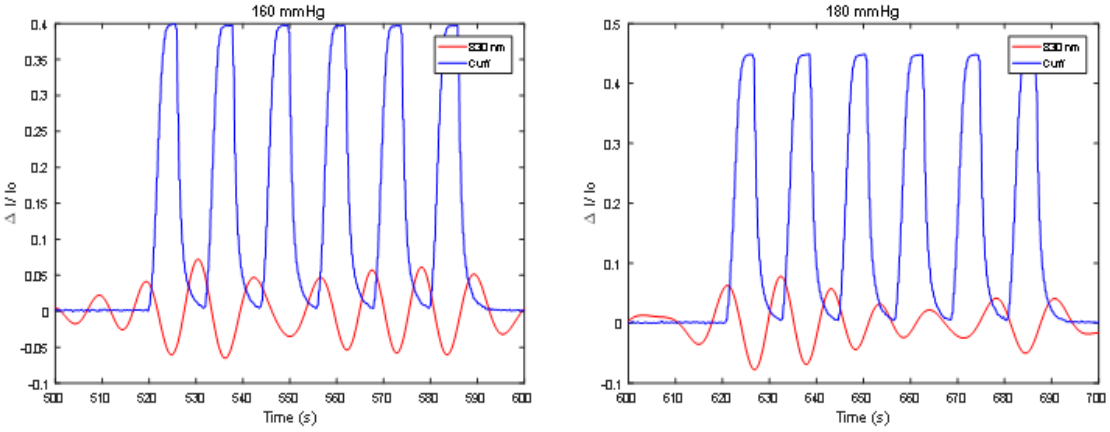

e f

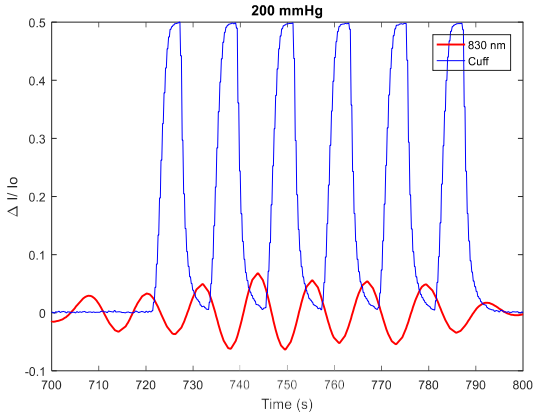

g

Figure 18. Represents a magnified version of cuff oscillations measured, band-pass filtered cerebral optical intensities at 830 nm, at each of the seven pressure occlusion periods,a.80, b.100,c.120,d.140,e.160,f.180, and g.200 mmHg for subject 1.

Certain cuff occlusion pressures elicited more coherent oscillations than others. This degree of coherence between the 690 nm and 830 nm oscillations was quantified using the phase synchronization index (PSI) for each inflation pressure. A PSI of 1 is obtained in the case of complete synchronization between the two signals and 0 when there is no synchronization. The PSI threshold, red line in Fig. 19, computed using the null statistic method (detailed in chapter 3), was 0.36. The PSI values obtained lie between 0 and 1 as seen in Fig. 19, with values closer to 1 indicating more coherent oscillations.

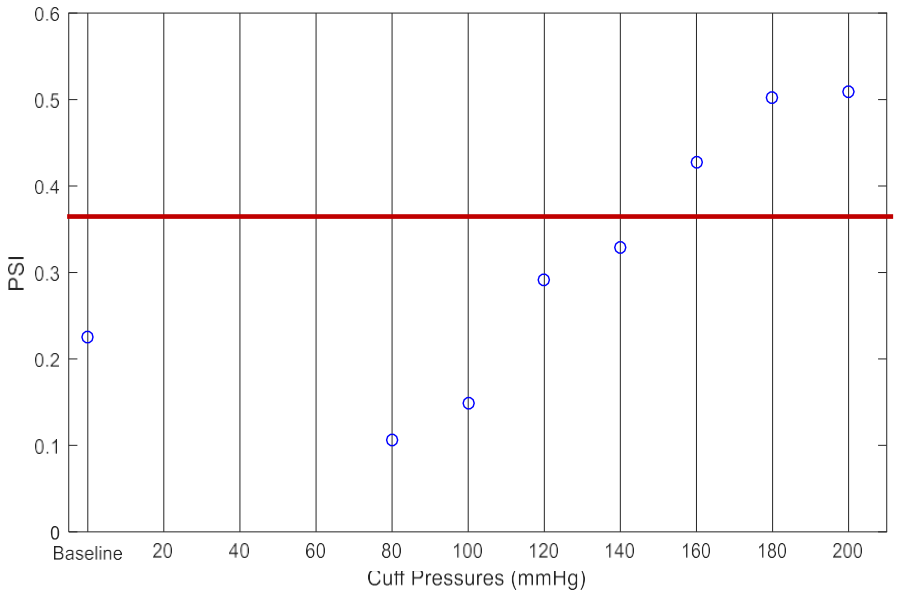

Figure 19. Details the PSI values obtained at each pressure value for subject 1. The PSI threshold (red line), computed using the null statistic method (detailed in chapter 3), was 0.36.

From the plot in Fig. 19, it can be interpreted that the pressure values 140, 160, 180, and 200 mmHg have been more efficacious in inducing coherent cerebral oscillations as compared to 80, 100, and 120 mmHg.

To further examine the significance of these results, the obtained PSI values for each subject were tested against a null hypothesis (explained in detail in chapter 3), obtained using phantom data, under the conditions of no phase synchronization between the two wavelength (690 and 830 nm) signals. Fig. 20 represents the p value for each PSI value computed against this null statistic. By considering a 5 % level of significance (depicted by the red line in Fig. 20), it was possible to confirm those pressure values that were successful in inducing a high level of coherent cerebral oscillations. There would be a 5 % probability of obtaining a PSI of 0.36 or greater in the absence of phase synchronization between the two measured cerebral optical intensity signals. Pressures 160,180, and 200 mmHg passed this threshold, as indicated by the red line in Fig. 20, however 140 mmHg did not.

Delpy et al., 1988

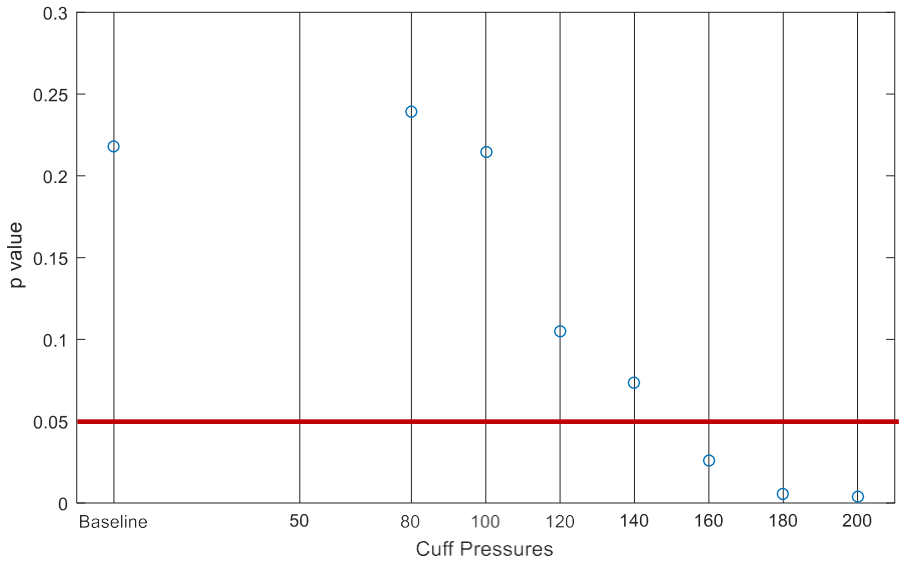

Figure 20. The p value for the PSI obtained at each pressure value for subject 1. The red line corresponds to an $\alpha = 0.05$.

Pressure (mmHg)	Baseline	80	100	120	140	160	180	200
PSI	0.2	0.1	0.2	0.3	0.3	0.4	0.5	0.5
p value	0.2	0.2	0.2	0.1	0.1	0.0	0.0	0.0

Table 1, summarizes the PSI between the optical intensities (690 nm and 830 nm) and p value obtained from subject 1 at each of the pressure values. Values are rounded off to two significant digits.

As indicated by the group averages of the two-thigh occlusion protocol results tabulated in Table 1, 180 and 200 mmHg were the most effective in inducing *Coherent* cerebral hemodynamic oscillations. Henceforth, the next portion of this study involving the varied cuff occlusion positions protocol, was performed at a concluded pressure value of either 180 mmHg or 200 mmHg.

4.2 VARIED CUFF POSITIONS WITH INFLATIONN AT THE OPTIMAL PRESSURE

The protocol lasted for 20 minutes and was conducted on three healthy subjects. The extracted oxy- and deoxy- hemoglobin time traces for subject 1, obtained from the measured cerebral optical intensity signals (at 690 and 830 nm) using modified Beer-Lambert law, are shown along with the cuff oscillations applied at a frequency of 0.0833 Hz in Fig. 21.

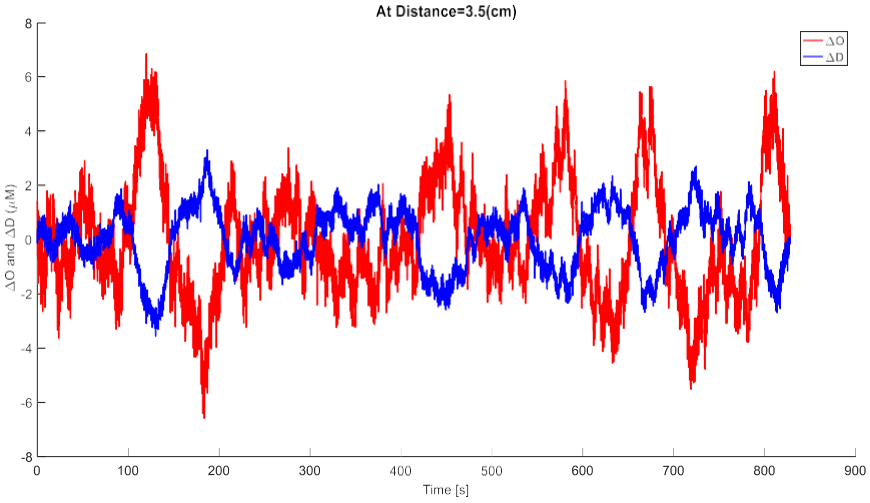

-

a.

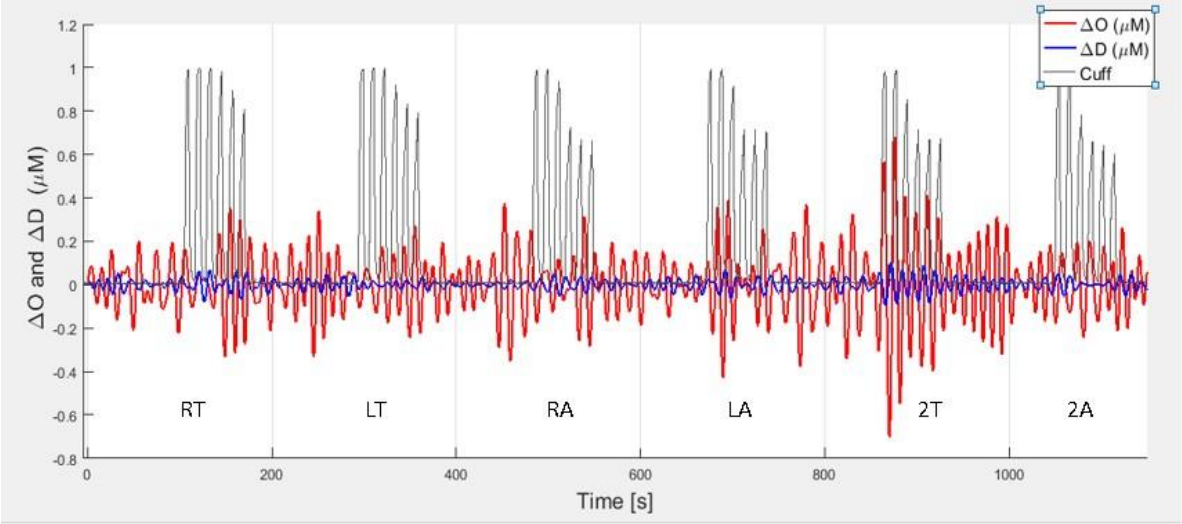

b.

Figure 21 **a**. Raw time traces of O(t) and D(t) extracted from the optical intensity traces collected at 690 nm and 830 nm. **b.** Band-pass filtered ($f_0 \pm 0.025$ Hz) O(t) and D(t) time traces, for subject 1, shown along with the cuff oscillations.

The occlusion positions were in the order of right thigh (RT), left thigh (LT), right arm (RA), left arm (LA), two thighs (2T), and two arms (2A).

Fig. 22, now represents a magnified version of the induced and extracted oxy- and deoxy- oscillations at each occlusion position.

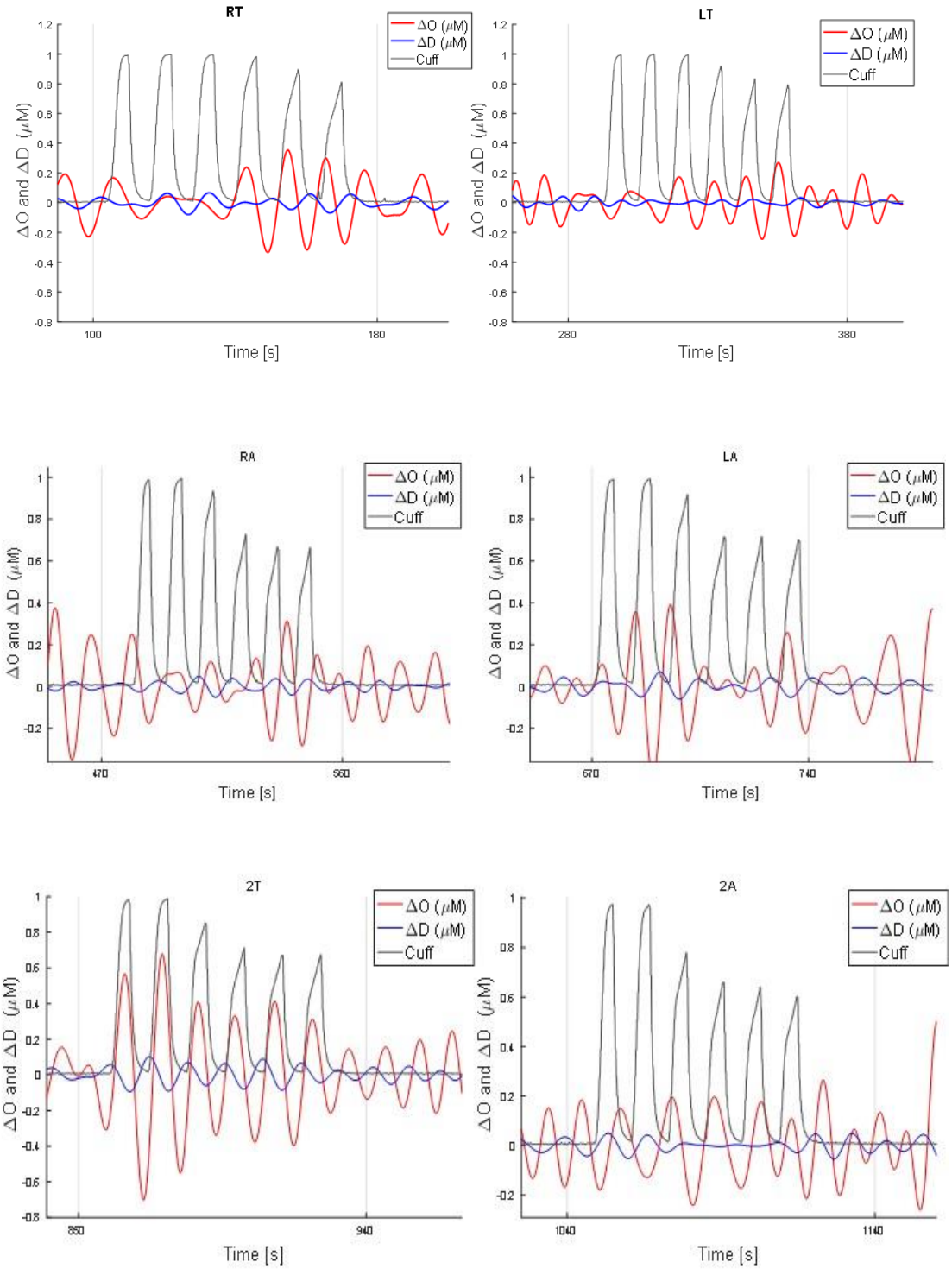

Figure 22. Magnified version of the filtered oxy- and deoxy- hemoglobin oscillations at each occlusion position along with the cuff oscillations.

It may be observed that the cuff oscillations are in phase with respect to the extracted oxy hemoglobin trace, as opposed to the measured cerebral optical intensity signals, which are out of phase with the cuff signal. This can be explained by the inverse proportionality relationship of the measured cerebral optical intensity signal with the extracted oxy- hemoglobin oscillations.

A better understanding of the cuff occlusion position that effectively induced coherent oscillations, can be obtained by examining the oscillations measured at each occlusion period in Fig. 22. The two thigh occlusion resulted in the oxy- and deoxy- hemoglobin traces being the most in and out of phase respectively, with the cuff oscillations. This was quantified by computing the PSI of the oscillations induced at different cuff positions, and plotted in Fig. 23. Only the two-thigh cuff occlusion position passed the PSI threshold = 0.6 (red line), determined using the null statistic method, with $\alpha = 0.05$, thereby concluding that occlusion at these cuff positions produced oscillations with more phase-lock.

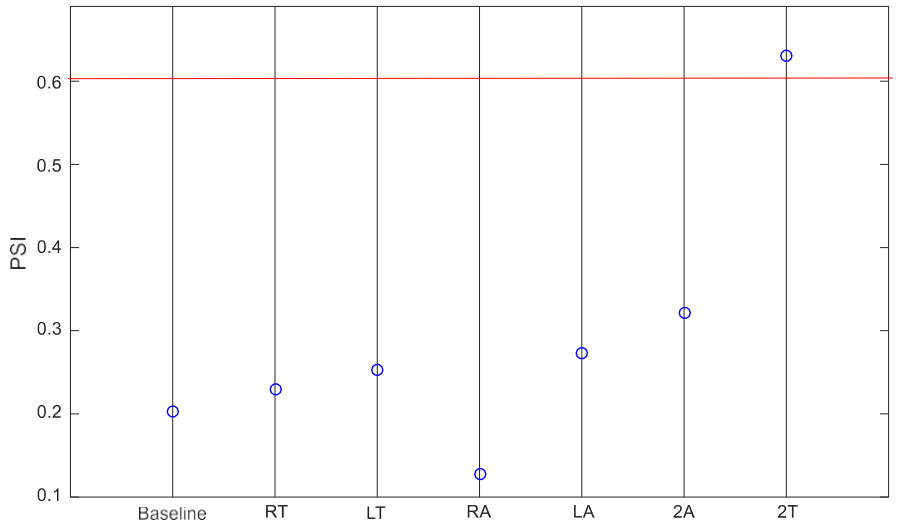

a.

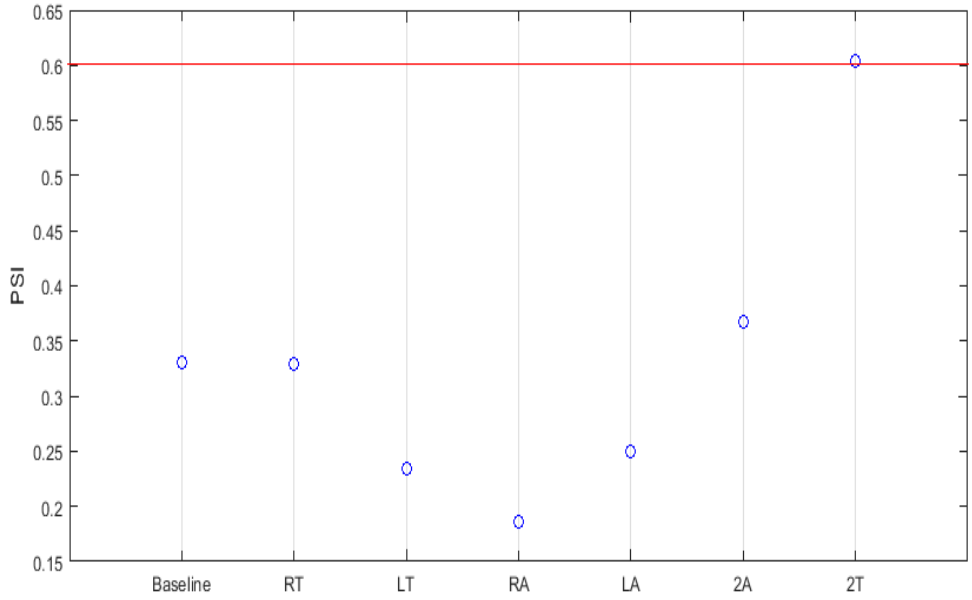

b.

Figure 23. Details the PSI values obtained at each occlusion position between the O(t) and D(t) time traces for,

a. Subject 1 b. Subject 2

The PSI threshold (red line), computed using the null statistic method (detailed in chapter 3), was 0.6.

The results were confirmed against the null statistic generated from phantom data, under the conditions of no phase synchronization between the extracted oxy (O(t)) and deoxy (D(t)) hemoglobin signals. Using $\alpha = 0.05$, the p value for each PSI value shown in Fig. 23, was calculated. There would be a 5 % probability of obtaining a PSI of 0.6 or greater in the absence of phase synchronization between the two extracted O(t) and D(t) signals.

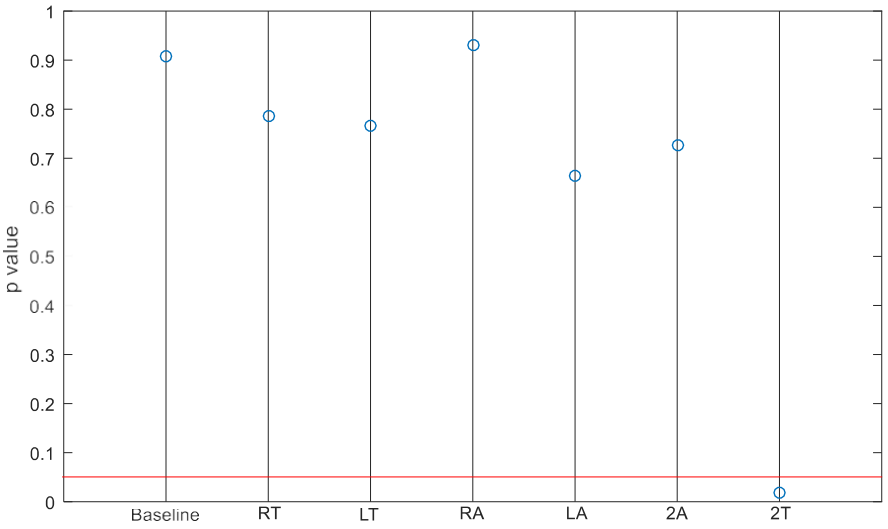

a.

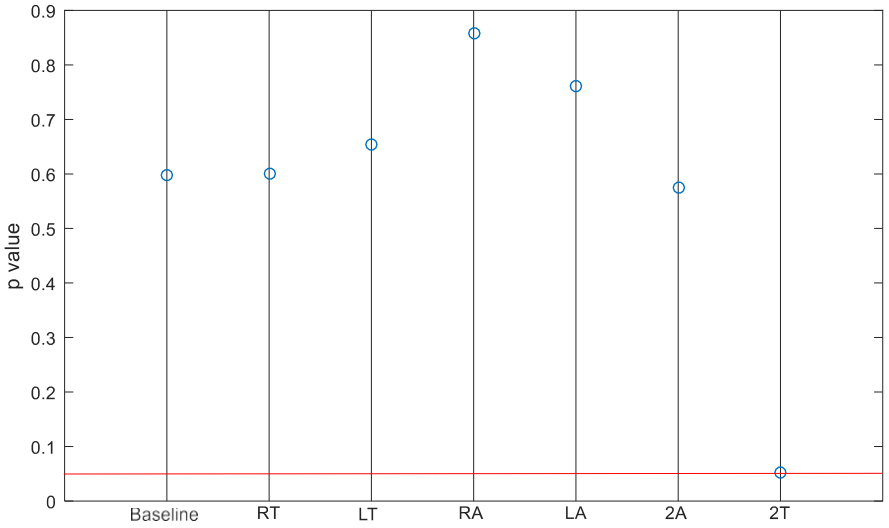

b.

Figure 24. The p value for the PSI obtained at cuff occlusion position value between the O(t) and D(t) time traces,

a. Subject 1
b. Subject 2

The red line corresponds to $\alpha = 0.05$.

From the plot shown in Fig. 24, it was established that the two-thigh cuff occlusion position induced highest coherence in cerebral hemodynamic oscillations.

Cuff-Positions	Baseline	Right Thigh	Left Thigh	Right Arm	Left Arm	Two Arms	Two Thighs
PSI	0.3±0.1	0.3±0.1	0.2±0.1	0.2±0.0	0.3±0.2	0.3±0.0	0.6±0.1
p value	0.8±0.2	0.7±0.1	0.7±0.1	0.9±0.1	0.7±0.1	0.7±0.1	0.0±0.0

Table 2, summarizes the group averages of PSI and p value obtained from 2 subjects at each of the cuff-occlusion positions. Values are given as the mean and standard error of the measurements across 2 subjects. Values are rounded off to two significant digits.

4.3 CONCLUSION AND FUTURE SCOPE

The intention of the results presented here was to interpret and conclude the suitability of measured factors for experimental protocols of Coherent Hemodynamics Spectroscopy (CHS). The primary focus of this research was to address questions pertaining to the optimization of experimental protocols for measurement and collection of CHS spectra. The importance lies in the fact that an optimally measured CHS spectra would allow for optimal application of the CHS model (Fantini. 2014), towards the quantification of model physiological parameters.

Quantification of pertinent features of measured oscillations using tools like Phase Synchronization Index (PSI), was used to conclude on results. A threshold for PSI was established, that is 0.36 for the optical intensities (690nm and 830 nm), and 0.6 when considering extracted O(t) and D(t) traces. This study allowed us to identify optimal pneumatic cuff conditions for CHS. It also provided an in depth understanding of the minimal conditions required to bring about changes in the human systemic system in response to pneumatic cuff based perturbations.

We found that a cuff occlusion pressure of at least 160 mmHg was required to induce significant changes in MAP, and elicit hemodynamic oscillations significant enough in terms of coherence, as indicated by Fig. 19. By studying and assessing cerebral hemodynamic oscillations elicited at each pressure (Fig. 18), we could conclude on certain pressures performing better than others. This helped in understanding the crucial role played by pressure of the pneumatic thigh cuffs, and

was implemented in future studies. Optimal positioning of pneumatic cuff based perturbations was the objective sought to be achieved by the next study. We established that the 2 thigh cuffs elicited highest *Coherent* hemodynamic oscillations, as shown in Fig. 23. Different cuff positions like the arms, thighs, and different cuff combinations, like single arm/thigh, 2 arms/thighs, were explored and assessed (Fig. 22).

While these exploratory results are promising, this study paves the way for future research, which could build upon these results to further enhance the characterization of CHS experimental protocols. For instance, the inclusion of additional accessories such as a tilt table (Lovell et al., 2000), to be a part of the CHS protocol. Depending on the degree of the table tilt, the cerebral blood volume could increase or decrease, thereby affecting the measured CHS spectra. Another area that could be explored is the subject's resting position, supine, sitting (currently employed position), or supine with head tilted at an angle, during the experimental protocol (Song et., 2015).

BIBLIOGRAPHY

- Bigio, Irving J., and Sergio Fantini. *Quantitative Biomedical Optics: Theory, Methods, and Applications*. Cambridge U Press, 2016.
- Cassot F., F. Lauwers, C. Fouard. S. Prohaska, and V. Lauwers-Cances. “A novel three-dimensional computer- assisted method for a quantitative study of microvascular networks of the human cerebral cortex.” *Microcirc* 13 (2006): 1-18.
- Fantini, Sergio. “A hemodynamic model for the physiological interpretation of in vivo measurements of the concentration and oxygen saturation of hemoglobin.” *Phys. Med. Bio.* 47.18 (2002): N249-57.
- Fantini, Sergio. "A new hemodynamic model shows that temporal perturbations of cerebral blood flow and metabolic rate of oxygen cannot be measured individually using functional near-infrared spectroscopy,." *Physiol. Meas.* 35 (2014): N1-N9.
- Fantini, Sergio. “Dynamic model for the tissue concentration and oxygen saturation of hemoglobin in relation to blood volume, flow velocity, and oxygen consumption: Implications for functional neuroimaging and coherent hemodynamics spectroscopy (CHS).” *NeuroImage* 85 (2014): 202-21.

- Fantini, Sergio, Dennis Hueber, Maria Angela Franceschini, Enrico Gratton, Warren Rosenfield, Phillip G. Stubblefield, Dev Maulik, Miljan R. Stankovic. " Non-invasive optical monitoring of the newborn piglet brain using continuous-wave and frequency-domain spectroscopy." *Physics in Medicine and Biology* 44.6 (1999): 1543-563.
- "Imagent™." www.iss.com. ISS, Inc.
- Kainerstorfer, Jana M., Angelo Sassaroli, Kristen T. Tgavalekos, and Sergio Fantini. "Cerebral autoregulation in the microvasculature measured with near-infrared spectroscopy." *Journal of Cerebral Blood Flow & Metabolism* 35 (2015): 959-66.
- Kainerstorfer, Jana M., Angelo Sassaroli, Michele L. Pierro, Bertan Hallacoglu, and Sergio Fantini. " Coherent hemodynamics spectroscopy based on a paced breathing paradigm – Revisited." *J. Innov. Opt. Health Sci.* 7 (2014): 9pp.
- Kainerstorfer, Jana M., Angelo Sassaroli, and Sergio Fantini. "Coherent hemodynamics spectroscopy in a single step." *Biomed. Opt. Express* 5 (2014): 3403-416.
- Lovell, Timothy A., MB, BS, FRCA, Alan C. Marshall, MB, BS, FRCA, Clare E., PHD, Martin Smith, MB, BS, FRCA, and John C. Goldstone, MD, FRCA. "Changes in Cerebral Blood Volume with Changes in Awake and Anesthetized Subjects." *Anesthesia & Analgesia* 90.2 (2000): 372-76.

- Mehta, Arpan R., John-Stuart Brittain, and peter Brown. “The Selective Influence of Rhythmic Cortical versus Cerebellar Transcranial Stimulation on Human Physiological Tremore.” *Journal of Neuroscience* 34.22 (2014): 7501-508.
- Pierro, Michele L., Jana M. Kainerstorfer, Amanda Civiletto, Daniel E. Weiner, Angelo Sassaroli, Beratn Hallacoglu, and Sergio Fantini. “Reduced speed of microvascular blood flow in hemodialysis patients versus healthy controls: A coherent hemodynamics spectroscopy study.” *Journal of Biomedical Optics* 19 (2014): 9pp.
- Pierro, Michele L., Bertan Hallacoglu, Angelo Sassaroli, Jana M. Kainerstrofer, and Sergio Fantini. “Validation of a novel hemodynamic model for coherent hemodynamics spectroscopy (CHS) and functional brain studies with fNIRS and fMRI.” *NeuroImage* 85(2014): 222-33.
- Ran, Cheng, Yu Shang, Don Hayes Jr., Sibu P. Saha, and Guoqiang Yu. “Noninvasive optical evaluation of spontaneous low frequency oscillation in cerebral hemodynamics.” *NeuroImage* 62.3 (2012): 1445-454.
- Sassaroli, Angelo, and Sergio Fantini. "Comment on the modified Beer-Lambert law for scattering media." *Phys. Med. Bio.* 49 (2004): N255-257.
- Sassaroli, Angelo, Yunjie Tong, Christian Benes, and Sergio Fantini. “Data analysis and statistical tests for near-infrared functional studies of the brain.” *Multimodal Biomedical Imaging III* 6850 (2008): 6pp.

- Song, Soohwa, Dohyun Kim, Dong Pyo Jang, Jongshill Ee, Hyon Lee, Kyoung-Min Lee, and In Young Kim.” Low-frequency oscillations in cerebrovascular and cardiovascular hemodynamics: Their interrelationships and the effect of age.” *Microvasc. Res.* 102 (2015): 46-53.
- Themelis, George, Helen D’Arceuil, Solomon G. Diamond, Sonal Thaker, Theodore J. Huppert, David A. Boas, and Maria Angela Franceschini. “ Near-Infrared Spectroscopy measurement of the pulsatile component of cerebral blood flow and volume from arterial oscillations.” *J. Biomed. Opt.* 12.1 (2007).
- Wihal, Sharon B., Chiara M. Polzonetti, Annamarie Stehli, and Enrico Gratton. “Phase synchronization of oxygenation waves in the frontal areas of children with attention-deficit hyperactivity disorder detected by the optical diffusion spectroscopy correlated with medication.” *J. Biomed. Opt.* 17.2 (2012).
- Zheng, Feng, Angelo Sassaroli, and Sergio Fantini. “ Phasor representation of oxy- and deoxyhemoglobin concentrations: what is the meaning of out-of-phase oscillations as measured by nearinfrared spectroscopy?” *J. Biomed. Opt.* 15.4 (2010).